Study on dryout point in vertical narrow annuli

TIAN Wen-Xi, AYE Myint, QIU Sui-Zheng, JIA Dou-Nan

(State Key Laboratory of Multiphase Flow in Power Engineering, Xi'an Jiaotong University, Xi'an 710049)

Abstract Prediction of dryout point is experimentally investigated with deionized water upflowing through narrow annular channel with 1.0 mm and 1.5 mm gap respectively. The annulus with narrow gap is bilaterally heated by AC current power supply. The experimental conditions covered a range of pressure from 0.8 to 3.5 MPa, mass flux of 26.6 to 68.8 $kg \cdot m^{-2} \cdot s^{-1}$ and wall heat flux of 5 to 50 $kW \cdot m^{-2}$. The location of dryout is obtained by observing a sudden rise in surface temperature. Kutateladze correlation is cited and modified to predict the location of dryout and proved to be not a proper one. Considering in detail the effects of geometry of annuli, pressure, mass flux and heat flux on dryout, an empirical correction is finally developed to predict dryout point in narrow annular gap under low flow condition, which has a good agreement with experimental data.

Keywords Narrow annular channel, Bilaterally heating, Dryout point, Critical quality, Annular flow

CLC numbers TL33, O359

1 Introduction

Various mechanisms for the onset of the critical heat flux (CHF) conditions have been proposed and they can roughly be classified into two categories: the departure from nucleate boiling (DNB) and the dryout of liquid film (DO).[1] From the point of view of engineering, the CHF caused by the latter mechanism is of particular importance since boiling annular flow is one of the most common flow patterns in gas-liquid two-phase flow and it occurs in a wide range of vapor quality of interest. This study deals with the CHF onset caused by liquid film dryout.

In forced convective boiling, dryout occurs when the heat flux is raised to such a high level that the heated surface can no longer support continuous liquid contact.[2] It is characterized by a sudden rise in the surface temperature. Due to poor heat transfer properties of the vapor, high heated surface temperature is often encountered in post-dryout region. Pressurized water nuclear reactors normally operate under conditions where dryout does not occur, however, dryout may occur during both blowdown and reflood phases of a LOCA. Furthermore, the knowledge of characteristics of dryout is very necessary to evaluate capabilities of the plant components such as the once-through steam generators.

Lots of study have been made on dryout and most of them were on conventional round tubes or rod bundles with high flow condition corresponding to the operating condition of Pressurized Water Reactor,[11-12] however, the available dryout data for annuli under low flow conditions are very limited. Even for these very few studys on annulus, the main interest is focused on internal heating corresponding to Pressure-Tube Reactor. Therefore, the experimental study on dryout point in bilaterally heated narrow annuli under low flow condition has been carried out in this study. The objective of this study is to expose the thermal-hydraulic characteristics when dryout occurs, discuss the influencing factors on dryout and finally get an empirical correlation for prediction of dryout in bilaterally heated narrow annuli.

2 Experimental apparatus

2.1 Test loop

The experiments were carried out in the test loop shown schematically in Fig.1. The experimental system consisted of a measuring and monitoring system and a circulating water test loop. The system is provided with the pressurizer, the pump, the calibrated

Received date: 2004-04-06

flow meter, the preheater, the test section and the cooler. Subcooled deionized water circulated by the pump, flowed through the system pipes, the flow meter, the pre-heater, then it is fed to the test section and flowed into the cooler where the fluid is condensed. The flow rate is regulated and maintained by the bypass and the valves.

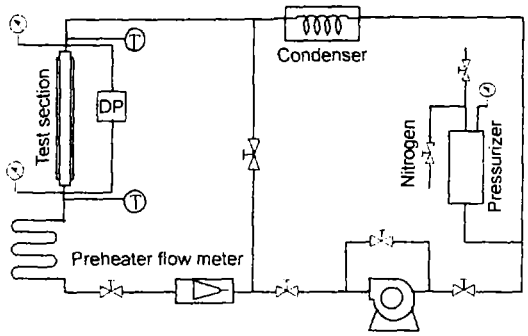

Fig.1 Schematic of the experimental apparatus.

2.2 Test section

A schematic diagram of the test section is shown in Fig.2. The test sections are made of specially processed straight stainless steel tubes with linearity error less than 0.01% to form narrow concentric annuli. The test section had the following geometrical parameters: length in 850 mm; 10 mm inner diameter of the outside tube, 8 mm and 7 mm outer diameter of the insidetube. Respectively, the corresponding annular gap size is then 1.0 mm and 1.5 mm. The test section is bilaterally heated by AC power supply, so it is very essential to ensure the concentricity and the electrical insulation between the outside tube and inside tube. Thus three small ceramic rods, 2.0 mm in diameter and 2.5 mm in length, are arranged at the same cross section with equal angular interval at the middle of test section as shown in Fig.3. A copper block is placed near the inlet to enhance the enthalpy to a required level. At the same time, to thermally insulate the test section from the environment, the whole test section is firstly covered by silicon-aluminium glass fiber 120 mm in thickness, a wire heater 3 kW in maximum power is wrapped outside of this heat insulator to compensate heat loss of the test section, and then another silicon-aluminium glass fiber 50 mm in thickness is wrapped outside of the wire heater.

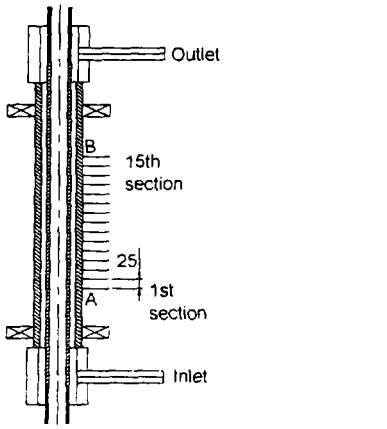

Fig.2 Schematic diagram of the test section (mm).

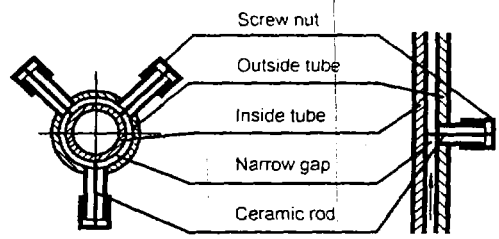

Fig.3 Schematic description of holding concentricity.

2.3 Parameters' measurement

The outer wall surface temperatures of the outside tube are measured by ϕ 0.5 mm thermocouples spot-welded on the surface at the axial intervals of 150 mm from the beginning of the heated section. Four thermocouples are arranged symmetrically on the horizontal cross section as shown in Fig.4. In order to determine the inner wall surface temperature of the inside tube, ϕ 0.5 mm sheathed thermocouple bundles are inserted into the inside tube at the same vertical level as the level of the thermocouples spot-welded on the outer surface of the outside tube. Two thermocouples are radially arranged in the thermal insulator to monitor the heat loss from the test section.

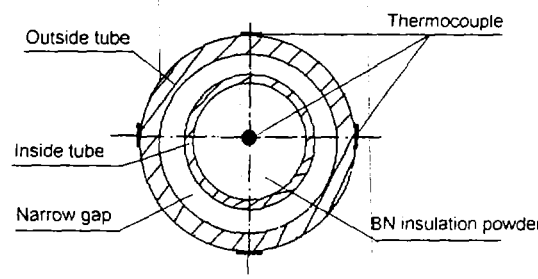

Fig.4 Thermocouple location on cross section.

2.4 Experimental uncertainties

All the measuring devices are calibrated by the authoritative institutes. The uncertainty of the flow

rate is estimated within an accuracy of ±2%, the absolute pressure with an accuracy of ±0.25%, the liquid temperature with an accuracy of ±0.75%, the wall temperatures with an accuracy of ±1.5%, voltage with an accuracy of ±0.2%, current with an accuracy of ±0.2% and the pressure drop with an accuracy of ±0.25%. The channel length and the diameter are determined within the accuracy of ±1%. The heat loss from the test section is estimated to be less than 3%.

3 Empirical correlation and modification

3.1 Kutateladze correlation

Former Soviet researcher Kutateladze (1979) proposed an empirical correlation used to calculate the critical quality (equilibrium quality where dryout occurs) for dryout occurring in round tube with 8 mm in diameter:

$$X_{DO,8} = 0.3 + 0.7e^{-45\omega} \tag{1}$$

$$\omega = \frac{G\mu_f}{\sigma\rho_f}\left(\frac{\rho_f}{\rho_g}\right)^{\frac{1}{3}} \tag{2}$$

If diameter of round tubes is different from 8 mm, the following correction factor C_1 is quoted to modify the above Eq.(1):

$$\left(\frac{0.008}{d_e}\right)^{0.15} = C_1, \quad X_{DO} = C_1 X_{DO,8} \tag{3}$$

3.2 Determination of the location of dryout

In flow boiling heat transfer regime, the temperature of the fluid is on the saturated level and the wall temperature also kept nearly a constant value. When dryout occurs, however, due to the poor heat transfer properties of the vapor, the wall temperature rises to a high level very rapidly. Then, the location detail of dryout point can be observed with the rapid change of temperature by using the thermocouples arranged in the test section.

From Fig.5(a) and Fig.5(b), it is easy to determine the location where dryout occurs: in Fig.5(a), dryout occurred only at the eleventh monitored section of inside tube, while in Fig.5(b), dryout occurred on the surfaces of both tubes. After obtaining the location detail of dryout points, via the heat balance, the critical quality can be written as follows:

$$X_{DO} = \frac{4\left(q_{wi}d_{io}l_i + q_{wo}d_{oi}l_o\right)}{GH_{fg}\left(d_{oi}^2 - d_{io}^2\right)} - \frac{\Delta H_i}{H_{fg}} \tag{4}$$

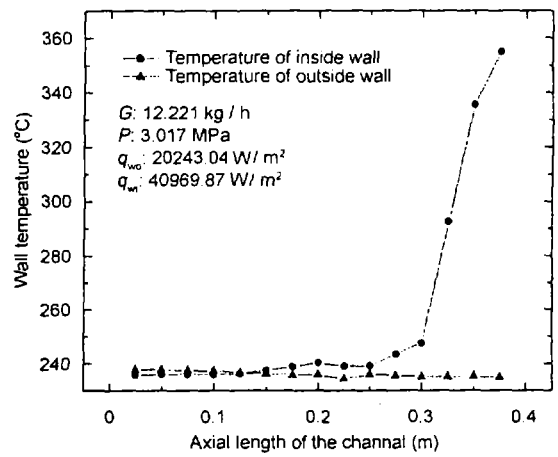

Fig.5(a) Schematic diagram of dryout occurring on the surface of inside tube.

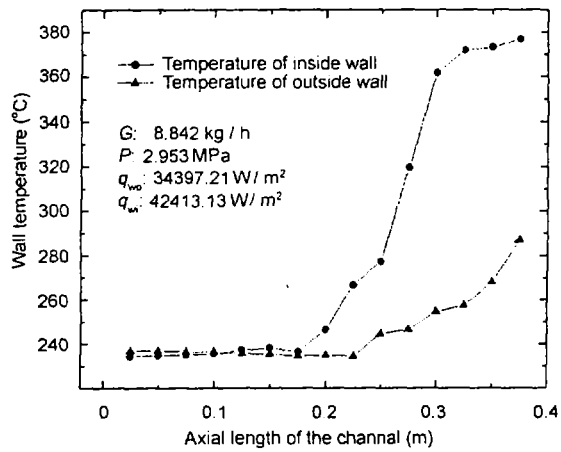

Fig.5(b) Schematic diagram of dryout occurring on both surfaces of both tubes.

3.3 Experimental data analysis

Total 211 data points are obtained among which 90 for 1.0 mm gap and 121 for 1.5 mm gap. The experimental conditions covered a range of pressure from 0.8 to 3.5 MPa, mass flux of 26.6 to 68.8 $kg \cdot m^{-2} \cdot s^{-1}$ and heat flux of 5 to 50 $kW \cdot m^{-2}$.

For liquid film on two sides, the tubes may not dryout at the same section. The data processing is handled respectively for inside tube and outside tube. Referring to Kutateladze correlation, the following form is adopted:

$$X_{DO} = C(0.3 + 0.7e^{-45\omega}) \tag{5}$$

where C is the linear fitting coefficient.

Based on this correlation, the linear fitting result are as follows:

For 1.0 mm gap size test section:

For inside tube:

$$X_{DO,i} = 1.4201(0.3 + 0.7e^{-45\omega}) \quad (6)$$

For outside tube:

$$X_{DO,o} = 1.4259(0.3 + 0.7e^{-45\omega}) \quad (7)$$

In a unified correlation for both side tubes:

$$X_{DO,av} = 1.4244(0.3 + 0.7e^{-45\omega}) \quad (8)$$

For 1.5 mm gap size test section:

For inside tube:

$$X_{DO,i} = 1.1973(0.3 + 0.7e^{-45\omega}) \quad (9)$$

For outside tube:

$$X_{DO,o} = 1.2626(0.3 + 0.7e^{-45\omega}) \quad (10)$$

In a unified correlation for both side tubes:

$$X_{DO,av} = 1.2307(0.3 + 0.7e^{-45\omega}) \quad (11)$$

Fig.6 shows the data handling results and the fitting curves. It is found from the figure that Kutateladze correlation (1) with correction factor (3) which is based on round tube underestimated the critical quality in narrow annuli, so it is absolutely necessary to take into account the effects of special geometry of narrow annuli and other parameters on dryout for a better prediction of dryout in narrow annuli.

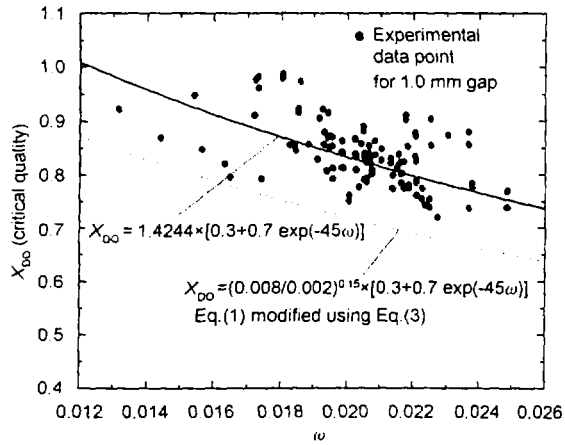

Fig.6(a) Fitting curves of experimental data for 1.0 mm gap test section.

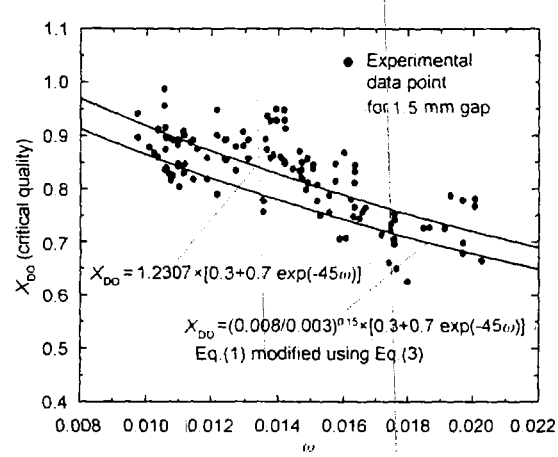

Fig.6(b) Fitting curves of experimental data for 1.5 mm gap test section.

4 Discussion

In the pre-dryout annular flow regime, the fluid flow consists of three components: the liquid film, the high-speed gas flow and the entrained liquid droplets. Parameters including evaporation of the liquid film, deposition of droplets and entrainment on the surface of the liquid film dominate the location of dryout and the corresponding critical quality.[17] The physical phenomena responsible for dryout in annuli are much more complex than those in tubes for its special geometry. In the reminder parts of this paper, the effects on the above flow parameters in annuli of geometrical structure, the size of the narrow annuli and the different wall heat flux on the tube at each side will be analyzed.

4.1 Effect of geometrical structure of annulus on dryout

For geometry different from round tubes, there exist the unbalance and asymmetry of fluid flow between both side tubes in annuli. In single-phase flow, in both laminar and turbulent flow regimes, the shearing force of outside tube acting on fluid τ_o is less than that of inside tube τ_i. This is also assumed to be true in two-phase annular flow at the vapour-liquid films interfaces.[14] And also the centrifugal force (this force must be considered for circumferential direction) always contributes to disengage of liquid droplets from inside tube to outside tube. So, just as shown in Fig.7, under the same heat flux and mass flux conditions, the liquid film on the surface of inside tube firstly dryout

and correspondingly the critical quality is less than that of outside tubes. As the centrifugal force and shearing force are related to the curvature of tubes, the value of the critical quality is assumed to related to the ratio of diameter of each side tube to the average diameter, just as the following Eq.(12):

$$X_{DO} \propto \left(\frac{r_j}{r_{av}}\right),$$

$$j=i,o$$

$$r_{av} = \frac{r_i + r_o}{2} \tag{12}$$

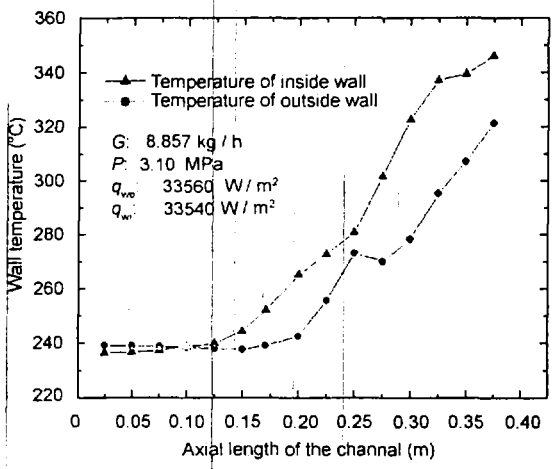

Fig.7 *Location of dryout point on both side tubes under the same condition.*

4.2 Effect of gap size of test section on dryout

Entrainment rate decreases with the gap size increasing, while deposition rate of droplets increases with gap size increasing. When dryout occurs in a narrower annular gap, because of the lower entrainment rate and the higher deposition rate, the quantity of the droplets is less and the drop sizes are smaller, thus the critical quality is higher. To take into account the effect of gap size, Eq.(3) is once quoted and proved to be not a proper one (Fig.6). The following Eq.(13) is finally adopted through the regression analysis of experimental data:

$$\left(\frac{0.008}{d_e}\right)^{0.335} = C_2, \quad X_{DO} = C_2 X_{DO.8} \tag{13}$$

4.3 Effect of different wall heat flux of each side tube on dryout

The fluid can be directly bilaterally heated with AC current power supply on each side tube. The different heat fluxes on each surface contribute much to the location of dryout and the critical quality. The heat flux dominates the evaporation rate of liquid film, on the other hand, it also has a great influence on the deposition rate of droplets because it causes the vapor flow normal to the heated wall. Under the same pressure and flow rate condition, for each of the two side tubes, the evaporation rate enhances and the liquid film drys-out earlier with increasing of the wall heat flux. So it is assumed that the critical quality is related to the ratio of average heat flux value to the heat flux on each side tube, just as the following Eq.(14):

$$X_{DO} \propto \left(\frac{q_{av}}{q_j}\right),$$

$$j=i,o,$$

$$q_{av} = \frac{q_i + q_o}{2} \tag{14}$$

4.4 Developed empirical correlation

Considering the effect of the above factors including geometry, gap size, wall heat flux as well as pressure and mass flux on the dryout quality, a multiple-regression analysis is adopted to analyze the experimental data. The final empirical correlation is written as Eq.(15):

$$X_{DO.j} = 0.533\left(\frac{r_j}{r_{av}}\right)^{0.083} \times \left(\frac{0.008}{d_e}\right)^{0.335} \times \left(\frac{q_{av}}{q_i}\right)^{0.096} \times \left(\frac{P}{10}\right)^{-0.016} \times \left(\frac{G}{100}\right)^{-0.346} \tag{15}$$

where j=i,o.

Fig.8 shows a good agreement between experimental and calculated data with an average error less than 5.0%, standard RMS error less than 6.7%, the measure of dispersion less than 7.1%.

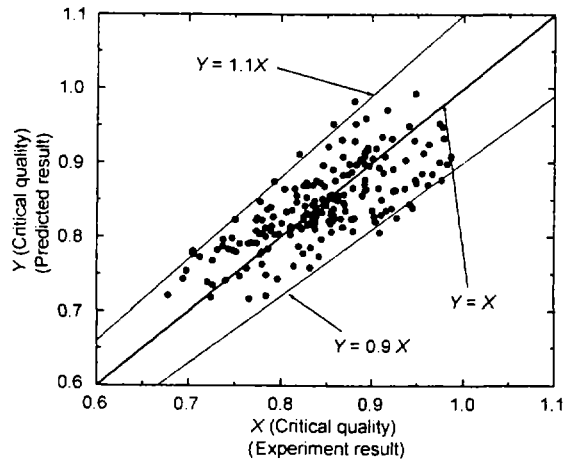

Fig.8 Comparison between experimental result and prediction of Eq.(15).

5 Conclusion

(1) Experimental study on dryout in vertical narrow annuli has been carried out under low flow condition. 211 data points were obtained for 1.0 mm and 1.5 mm annular gap size of test section.

(2) Kutateladze correlation based on round tubes was quoted and modified to be applied for annuli, however was found not suitable for narrow annuli under low flow conditions.

(3) Considering the influencing factors such as geometry of test section, pressure, mass flux, heat flux etc., an empirical correlation is developed to suit to bilaterally heated annuli and it had a good agreement with experimental data.

(4) Due to its particular structure geometry, mechanism of dryout in narrow annuli is found to be more complex than that of conventional round tubes and further study should be carried out.

Nomenclature

d hydraulic diameter (m)
d_e equivalent diameter (m)
d_{oi} inner diameter of outside tube (m)
d_{io} outer diameter of inside tube (m)
e exponent
G mass flux ($kg \cdot m^{-2} \cdot s^{-1}$)
H enthalpy ($kJ \cdot kg^{-1}$)
H_{fg} latent heat of vaporization ($kJ \cdot kg^{-1}$)
ΔH_i inlet subcooled enthalpy ($kJ \cdot kg^{-1}$)
l length of channel (m)
P pressure (MPa)
q_{wi} heat flux on the surface of inside tube ($kW \cdot m^{-2}$)
q_{wo} heat flux on the surface of outside tube ($kW \cdot m^{-2}$)
r_{oi} inner radius of outside tube (m)
r_{io} outer radius of inside tube (m)
X vapor quality

Greek symbols

ρ density ($kg \cdot m^{-3}$)
μ dynamic viscosity ($N \cdot s \cdot m^{-2}$)
σ surface tension ($N \cdot m^{-1}$)

Subscripts / Superscripts

av average
DO Dryout Point
f saturated liquid
g saturated vapor
i inside tube or inlet
o outside tube
w wall surface

References

1 Tomio Okawa, Akio Kotani, Isao Kataoka. Prediction of dryout heat flux in vertical round tubes with uniform and non-uniform heating. The 10th international topic meeting on nuclear reactor thermal hydraulics, October, 2003, Seoul, Korea.

2 Cheng J C, Ozkaynak F T, Sundaram R K. Nuclear Engineering and Design, 1979, **51**: 143-155.

3 Chen Zhihang, Cao Bolin. Two phase flow and heat transfer (in Chinese). Beijing: Mechanical Industry Press, 1983.

4 Knudsen J G, Katz D L. Fluid dynamics and heat transfer. New York: McGraw-Hill, 1958: 186-195.

5 Lee Kwang-Won, Baik Se-Jin, Ro Tae-Sun. Nucl Eng Design, 2000, **200**: 69-81.

6 Levy S, Healzer J M, Abdollahian D. Nucl Eng Design, 1981, **65**: 131-140.

7 Doerffer S, Groeneveld D C, Cheng S C. Nucl Eng Design, 1997, **177**: 105-120.

8 Katto Y. International Journal of Heat Mass Transfer, 1984, **27**: 83-891.

9 Venkateswararao P, Semiat R, Dukler A E. International Journal of Multiphase Flow, 1982, **8**: 509-524.

10 David D H, Issam M. International Journal of Heat Mass Transfer, 2000, **43**: 2573-2604.

11 Tippets F E. Trans Am Soc Mech Eng J Heat Transfer, 1964, **86C** (1): 23-38.

12 Chun Se-Young, Chung Heung-June *et al*. Nucl Eng Design, 2001, **203**: 159–174.